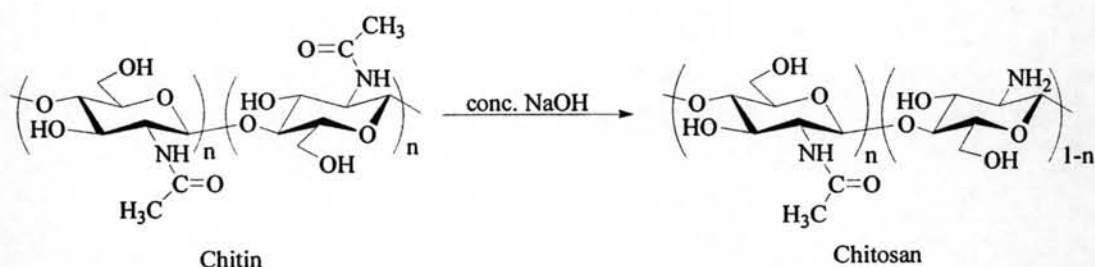


## CHAPTER II

### THEORY AND LITERATURE REVIEW

#### 2.1 Chitosan

Chitosan, a linear polycationic biopolymer, is prepared by alkaline *N*-deacetylation of chitin. Chemical structures of chitin and chitosan are shown in Scheme 2.1. Chitosan mainly consists of 2-amino-2-deoxy-D-glucose (GlcN) repeating unit with a small amount of 2-acetyl-2-deoxy-D-glucose residues. The amount of GlcN unit in chitosan is generally referred to the percentage degree of deacetylation or % DD, influencing its physical, chemical properties as well as biological activities. Various techniques can be used for determination of % DD such as IR [13], NMR [14], and pH-potentiometric titration [15].

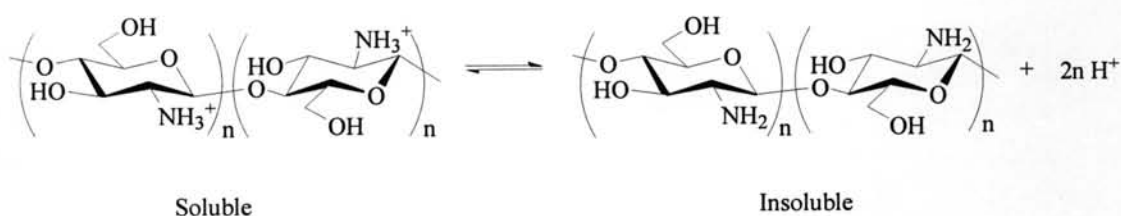


**Scheme 2.1** Structures of chitin and chitosan.

As a natural renewable resource, chitosan has a number of unique properties such as the physical, chemical, mechanical and biological properties including antimicrobial activity, nontoxicity, and biodegradability, which attract scientific interest in such fields as biotechnology, pharmaceuticals, cosmetics, agriculture, food science, and textiles. Due to its reactive amino and hydroxyl groups, chemical modification of chitosan to achieve its derivatives is used to expand its application.

## 2.2 Charged Derivatives of Chitosan

Generally, chitosan is soluble in aqueous medium in the presence of a small amount of acids such as acetic acid, lactic acid and so on. Chitosan can dissolve in aqueous acidic medium below pH 6.5; it precipitates above this pH due to lost its cationic nature. Importantly, chitosan's  $pK_a$  is near neutrality [16-20], and the soluble-insoluble transition occurs at pHs between 6 and 6.5 (Scheme 2.2). The application of chitosan was thus limited owing to the insolubility in neutral or high pH region.

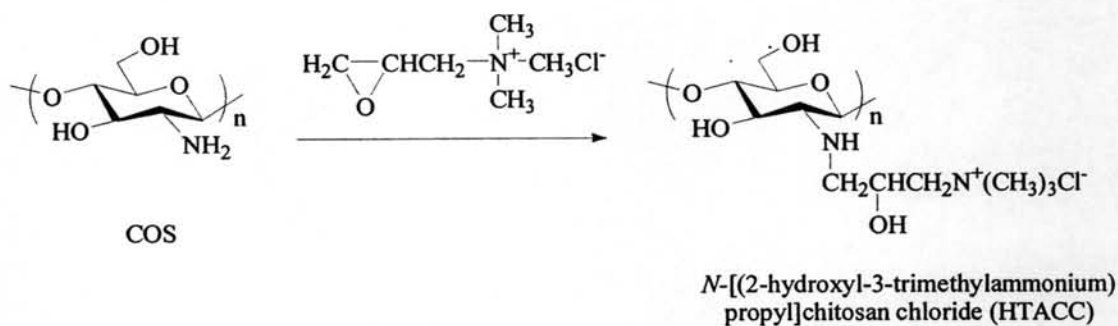


**Scheme 2.2** Soluble and insoluble form of chitosan in water.

To improve the solubility property, one effective way is to introduce charged functional groups to native chitosan. Chitosan has both reactive amino and hydroxyl groups, which can act as versatile functional groups for chemical modification under mild reaction conditions. The present research group is interested in introducing three charged functional groups, quaternary ammonium group, succinyl group and sulfonate group which impart chitosan to dissolve in neutral and high pH media. The following related research publications have been reported on chemical modification by grafting both three charged functionalities to the amino and/or hydroxyl groups.

In 2000, Seong *et al.* [7] synthesized a derivative of chito-oligosaccharide (COS), *N*-(2-hydroxy)propyl-3-trimethyl ammonium chitosan chloride (HTACC), using a reaction of glycidyltrimethylammonium chloride (GTMAC) (Scheme 2.3) and prepared COS by depolymerization of a fully deacetylated chitosan. The complete substitution of  $\text{NH}_2$  in COS with GTMAC was obtained at a four-to-one mol ratio of GTMAC to  $\text{NH}_2$  in COS in 18 h at 80°C in the presence of acetic acid.

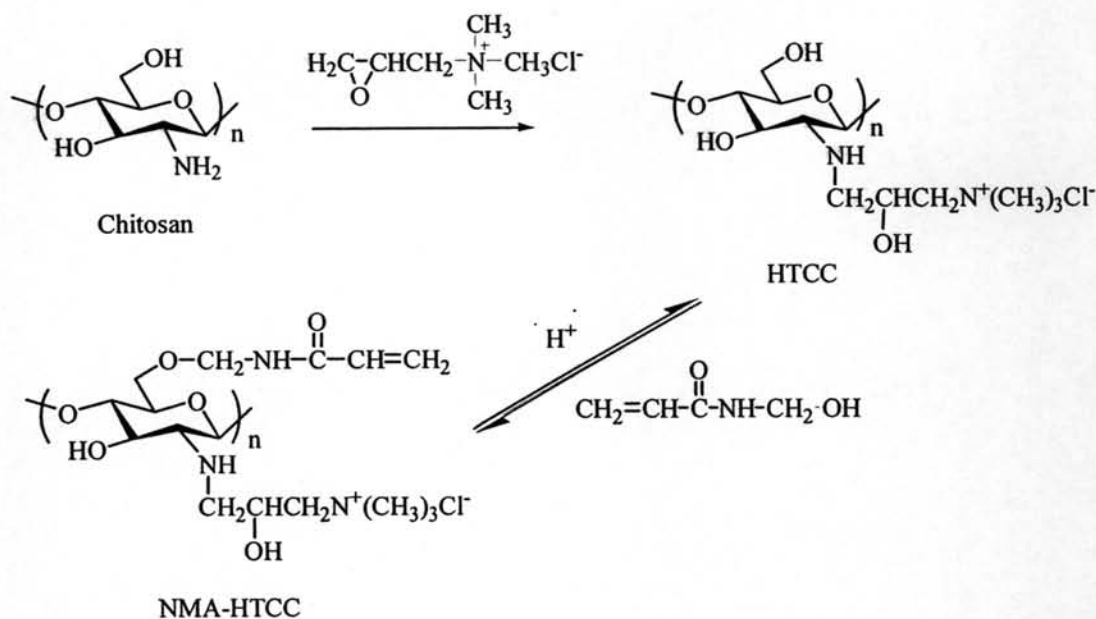
HTACC showed superior antimicrobial activity to COS due to the quaternary ammonium group from the substitution of  $\text{NH}_2$  in COS with GTMAC and therefore they were applied to the cotton fabrics.



**Scheme 2.3** Synthesis of *N*-[(2-hydroxy-3-trimethylammonium)propyl]chitosan chloride (HTACC) [7].

In 2003, Kim, *et al.* [21] synthesized a derivative of chito-oligosaccharide (COS) with quaternary ammonium functionality (HTACC) and studied its antimicrobial activity against *Streptococcus mutans* (*S. mutans*); a principal etiological agent of dental caries in humans. The resulting HTACC exhibited the growth inhibition of above 80% against *S. mutans* after 5 h, whereas chitosan showed the growth inhibition of above 10%. It was found that the antimicrobial activity of COS could be considerably enhanced by the introduction of quaternary ammonium functionality.

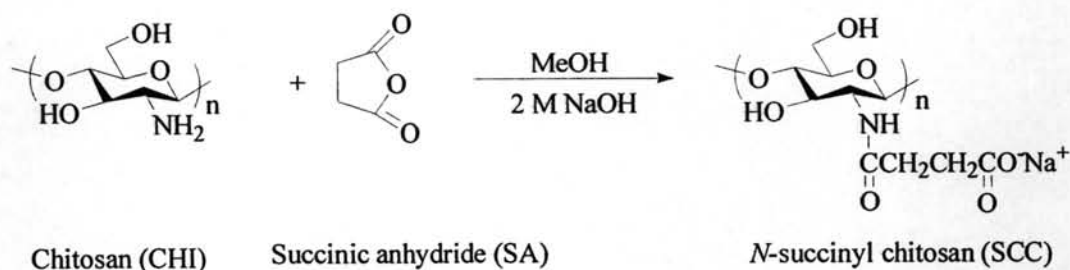
In 2004, Lim, *et al.* [8] reported a use of water-soluble chitosan derivative, *N*-[(2-hydroxy-3-trimethylammonium)propyl]chitosan chloride (HTCC), which was prepared by reacting chitosan with glycidyltrimethylammonium chloride (GTMAC). The HTCC was further modified by reacting with *N*-methyloylacrylamide (NMA) to prepare a fiber-reactive chitosan derivative, *O*-acrylamidomethyl-HTCC (NMA-HTCC) (Scheme 2.4). The NMA-HTCC has an excellent antimicrobial activity against both *S. aureus* and *E. coli* as compared to chitosan, which does not dissolve in pH 7.2 and does not show any antimicrobial activity under this condition.



**Scheme 2.4** Synthesis of HTCC and NMA-HTCC [8].

In 1999, Sashiwa, *et al.* [22] prepared *N*-acylated partially deacetylated chitin (DAC-88) derivatives via ring-opening reactions with various cyclic acid anhydrides and *N*-alkylation of DAC-88 were performed with various aldehydes, monosaccharides and disaccharides in an aqueous MeOH system.  $^1\text{H}$  and  $^{13}\text{C}$  NMR spectroscopies were used to characterize all products. The *N*-acylated and *N*-alkylated chitosan derivatives having carboxyl and sulfate group showed the solubility at the basic pH region. Some of chitosan derivatives substituted with saccharides showed the solubility at all pH ranges.

In 2003, Aoki, *et al.* [23] prepared chitosan bearing CD-P from *N*-succinyl chitosan (Suc-Chitosan) (Scheme 2.5), a hydrophilic polymer with reactive amino and carboxyl groups. These functional groups are available for connecting the cyclodextrins moieties (CDs) and showed the potential to remove toxic compounds from water.



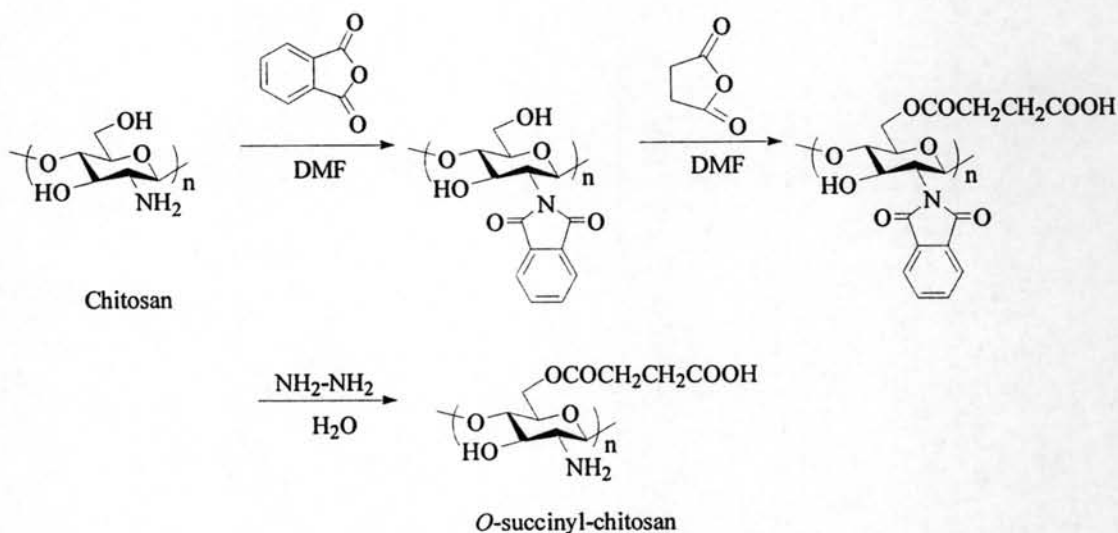
**Scheme 2.5** Synthesis of *N*-succinyl chitosan (SCC) [23].

In 2004, Kato, *et al.* [9] prepared a drug carrier, *N*-succinyl chitosan (Suc-Chi), by introduction of succinyl groups into chitosan *N*-terminal of glucosamine units. The Suc-Chi was conjugated by direct coupling of mitomycin (MMC) using carbodiimide (EDC). The conjugates of MMC with Suc-Chi showed good antitumour activities against various tumours. The Suc-Chi can function well as a drug carrier due to a long systemic retention, low toxicity and accumulation in the tumor tissue.

In 2006, Aiping, *et al.* [24] developed a simple and novel approach to synthesize the *N*-succinyl-chitosan (NSCS). FTIR,  $^1\text{H}$  NMR, element analysis and XRD were used to characterize the NSCS. It can be self-assembly of well-dispersed and stable nanospheres in distilled water. Transmission electron microscopy (TEM) was used to investigate the morphology of the nanospheres. The steady-state fluorescence spectroscopy indicates that the hydrophobic domain has been formed within these NSCS nanospheres. The *in vitro* cell culture demonstrates that NSCS is non-toxic and cell-compatible. It can be safely used as the drug matrix.

In 2007, Aiping, *et al.* [25] synthesized *N*-succinyl chitosan (NSCS) via ring opening polymerization of succinic anhydride. The interactions between NSCS and bovine serum albumin (BSA) were characterized by circular dichroism (CD), isothermal titration calorimetry (ITC), ultraviolet (UV) spectroscopy, fluorescence spectroscopy and transmission electron microscopy (TEM). This study demonstrates the potential of NSCS matrix for encapsulation of protein and other hydrophilic bioactive drugs.

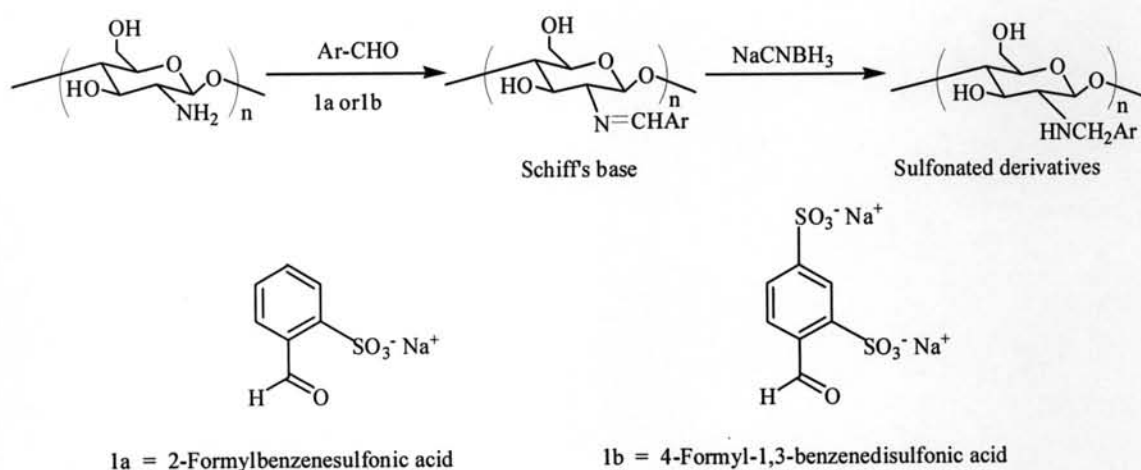
In 2003, Zhang, *et al.* [26] synthesized and characterized a novel water soluble chitosan derivative, *O*-succinyl-chitosan (Scheme 2.6), by one three-step reaction using phthaloyl group as the protection group for the amino group of chitosan and using hydrazine hydrate to remove the protective group. FTIR,  $^1\text{H}$  NMR,  $^{13}\text{C}$  NMR and elemental analysis were used to characterize the chemical structure of the modified chitosan. The modified chitosan shows much better solubility in water and the study of enzymatic degradation exhibited that the *O*-succinyl-chitosan was of low susceptibility to lysozyme and may have potential applications in a biomedical system.



**Scheme 2.6** Synthesis of *O*-succinyl chitosan [26].

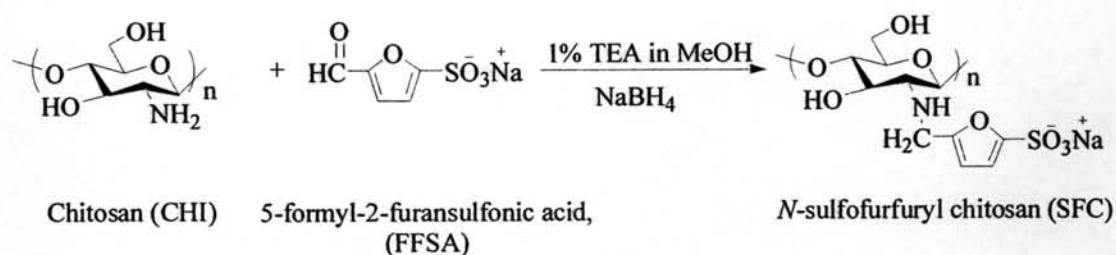
In 1992, Muzzarelli [27] prepared *N*-sulfofurfuryl-chitosan and sulfoethyl *N*-carboxymethyl chitosan by reacting chitosan with the sodium salt of 5-formyl-2-furansulfonic acid and 2-chloroethanesulfonic acid, respectively. The  $^{13}\text{C}$  NMR and FTIR spectra showed typical signals of furane carbons. Circular dichroism measurements were used to indicate its polyampholyte nature. The chelating reaction with metal ion was used to prove the chelating ability.

In 1997, Grégorio *et al.* [28] synthesized *N*-benzyl sulfonated derivatives of chitosan by reactions with 2-formylbenzene sodium sulfonate and 4-formylbenzene sodium disulfonate in the presence of sodium cyanoborohydride (Scheme 2.7). One-dimensional and two-dimensional NMR spectroscopies were used to characterize the structure of both products.



**Scheme 2.7** Synthesis of sulfonate derivatives of chitosan [28].

In 1998, Amiji [10] synthesized an amphoteric derivative of chitosan, *N*-sulfofurfuryl chitosan (Scheme 2.8), by reductive alkylation using the sodium salt of 5-formyl-2-furansulfonic acid as a reagent. The synthesized sulfonated chitosan was found to be soluble in aqueous medium over a wide pH range. *In vitro* blood compatibility of the sulfonated chitosan was evaluated by measuring the number of adherent platelets and the extent of platelet activation. The sulfonated chitosan appeared to possess non-thrombogenic properties and may be suitable for some blood-contacting applications.



**Scheme 2.8** Synthesis of *N*-sulfofurfuryl chitosan [10].

In 2002, Vongchan, *et al.* [11] synthesized sulfated chitosan from chitin which was derived from the shells of rice-field crabs under semi-heterogeneous conditions. The sulfated chitosan showed strong anticoagulant activity similar to heparin.

In 2006, Jayakumar, *et al.* [29] reviewed about the different synthetic methods of preparation of sulfated chitin and chitosan and their applications. They found that chemical modification would not change the fundamental skeleton of chitin and chitosan. The sulfated chitin and chitosan have a variety of applications such as adsorbing metal ions, biomedical, antimicrobial and drug delivery. They suggested that these materials have a potential for biomedical applications as a result of cell growth efficiency.

### 2.3 Polymer Adsorption

Adsorption of polyelectrolyte is governed by a complex interplay between molecular weight, solvent quality, interaction energy between the monomers and surface, the polyelectrolyte charge, the surface charge and the ionic strength. The usual description of conformations at an adsorbing interface is in terms of three types of subchains: trains, which have all their segments in contact with the substrate, loops, which have no contacts with the surface and connect two trains, and tails which are non adsorbed chain ends are shown in Figure 2.1 [30].



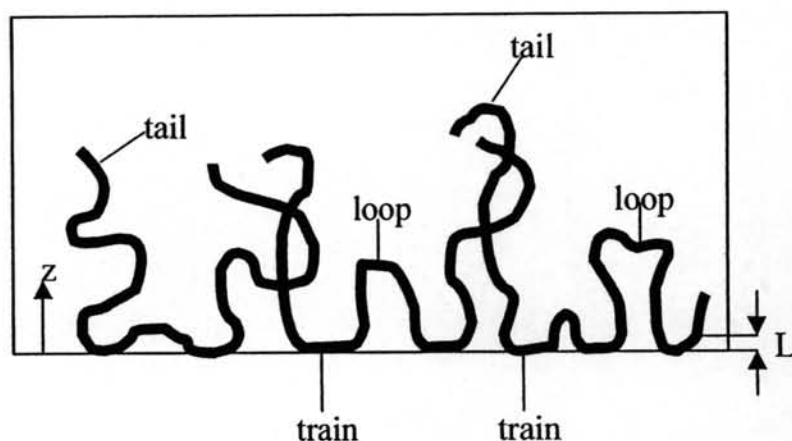


**Figure 2.1** Pictorial representation of an adsorbed polymer layer, indicating loops, tails and trains ( $L$ : thickness of chain) [30].

The amount of weak polyelectrolyte adsorbed depends strongly on charge density, controlled by ionic strength and pH. If the polyelectrolyte is fully charged, the adsorption layer is thin (trains with few loops and tails) and electrostatic repulsion opposes further adsorption. Increasing salt concentration reduces this repulsion, more polymers adsorb and the layer becomes thicker and also more extended. The adsorption also increases with increasing molecular weight of the polymer. Polymer segments tend to form more loops, tails and eventually extended chains as the adsorbed amount and layer thickness increase. At very high ionic strength, however, where all charges on polymer segments are completely screened, a more random coil-like conformation with a smaller radius of gyration is more favorable than the extended chain.

#### 2.4 Layer-by-Layer Adsorption

The fabrication of ultrathin polymer films on modified surfaces of material is important for various scientific and biological fields in order to modify the intact characteristics of these surfaces exposed to biological systems. In most cases, the material characteristics seem to be governed by the chemical composition of the surface. Coating a substrate surface with polymeric ultrathin films can maintain the original mechanical properties and/or fine structure of the substrate.

The technique of layer-by-layer (LBL) assembly discovered by Decher and co-workers [1] has been employed in wide areas, such as biosensors, separation or dialysis membranes, optical devices, surface modification, due to its simplicity and versatility [31-38]. This technique is based on the consecutive adsorption of polyanions and polycations via electrostatic interactions (Figure 2.2). The electrostatic attraction between positively and negatively charged molecules seems to be good choice as a driving force for multilayer build up [1]. As compared with the classic chemical immobilization method, such as hydrolysis, grafting technique, plasma treatment, ozone oxidation, entrapment of a polymer, coating of natural polymers, the LBL technique has the least demand for chemical bonds. The multilayers built by the LBL method afford a more stable coating than that prepared by physical adsorption because of the electrostatic attractions between layer to layer and layer to substrate. One important feature of this method is the adsorption at every step of polyanion/polycation assembly, which results in recharging of the outermost layer during the film fabrication process. The overcompensating adsorption, more than the equal charge, allows for charge reversal on the surface, which has two important consequences [1]: first, repulsion of equally charged molecules and thus self-regulation of the adsorption and restriction to a single layer; and second, the ability of an oppositely charged molecule to be adsorbed in a second step on top of the first one. The adsorption behavior of polyelectrolytes is influenced by factors such as the charge density [39], the ionic strength or the pH of the solutions and the solvent quality [40].

The process has many important advantages over other techniques for preparing ordered multilayer thin films; for example, the assembly is based on spontaneous adsorption and no stoichiometric control is necessary to maintain surface functionality, the assembled molecular films exhibit a much larger thermal and mechanical stability and can be prepared up to hundreds of layers, and so on [41]. Most of all, the process is easy and procedure can be adapted almost with any type of surface as long as surface charges are present, which is an ideal approach for use in biomedical applications.

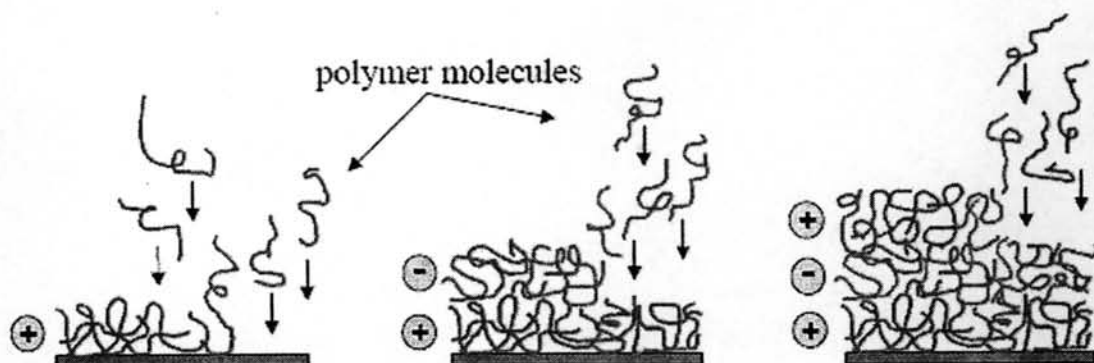


**Figure 2.2** The schematic representation of the layer-by-layer adsorption process [42].

## 2.5 Cellular Responses

Cell adhesion, spreading and migration on substrates are the first sequential reactions when coming into contact with a material surface, which is crucial for cell survival. The cellular behaviour on biomaterials is an important factor for evaluation of the biocompatibility of a biomaterial [43]. When foreign materials come into contact with body fluid or cell culture medium, the initial response is protein adsorption atop the materials' surfaces. Thus, the materials interact with the cells through the adsorbed protein layer. The composition and structure of this protein layer play critical roles in determining subsequent cell behaviors [44].

Mechanisms of cellular interaction with the environment are of paramount significance for biomimetic material development. There are two major categories of cell-biomaterial interactions: specific and unspecific. Unspecific interactions are usually difficult to control, because they are based on properties common to multiple cell types. These common cell characteristics include, for example, cell surface properties, such as the negative charge of the cell membrane, as well as ubiquitous lipophilic membrane proteins or lipophilic proteins of the extracellular matrix (ECM) that mediate unspecific adhesion to polymer surfaces. Specific interactions, in contrast, are much more controllable as they are primarily related to the interactions of defined chemical structures, such as ligands that interact with their corresponding cell surface receptors [45].

The dominance of the biorecognition process on cell behaviors, two main strategies in surface engineering of biomaterials are often employed. Firstly, the material surface properties such as chemical composition, hydrophilicity/hydrophobicity, surface charge and roughness, etc. are modulated to a state that the adsorbed proteins can maintain their normal bioactivities. This method, however, cannot induce specific cell behaviors due to the nonspecific protein absorption. The second strategy is to directly immobilize certain biomolecules on the biomaterial surfaces to induce specific cellular responding [46].

Cell adhesion involves a sequence of four steps: cell attachment, cell spreading, organization of an actin cytoskeleton, and formation of focal adhesions as shown in Figure 2.3 [47,48]. Following cell attachment, cells are sufficiently associated with the material to withstand gentle shear forces, whereas during the second phase, the cell body becomes flat and its plasma membrane spreads over the substratum. Thereafter, actin organizes into microfilament bundles that form an actin cytoskeleton. A fourth effect is the formation of focal adhesion that links the extracellular matrix (ECM) to the actin cytoskeleton. A great number of signaling events following the formation of focal adhesion are known [49].

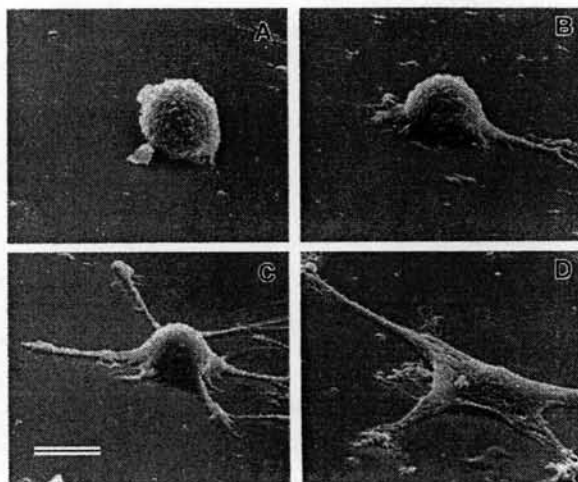


**Figure 2.3** Process of cell attachment to cell spreading. Scanning electron micrographs of adherent cells on substrates: A spheroid cells with no filapodial extensions; B spheroid cells with one to two filapodial extensions; C spheroid cells with greater than two filapodial extensions; D flattened morphology representative of well spread cells [48].

Up to now, there are many research publications reported the use of the LBL adsorption to prepare ultrathin polymer film for biomedical applications.

In 2000, Guy, *et al.* [50] investigated the interaction between poly(styrene sulfonate) (PSS) and poly(allylamine hydrochloride) (PAH) multilayers with human serum albumin (HSA). The results showed that the underlying complexity of concentration and pH dependent adsorption/desorption equilibrium often simply termed "protein adsorption" was the result of antagonist competing interactions that were mainly of electrostatic origin.

In 2003, Boura, *et al.* [51] prepared two types of polyelectrolyte multilayer films: poly(sodium-4-styrenesulfonate)/poly(allylamine hydrochloride) (PSS/PAH) and poly(L-glutamic acid)/poly(L-lysine) (PGA/PLL). The results showed that polyelectrolyte multilayered films enhanced cell attachment as similar to that on TCPS. Among the different coating tested, the film ending by PSS/PAH exhibited an excellent cellular biocompatibility and appeared to be the most interesting surface in terms of cellular adhesion and growth, thereby constituting an excellent material for endothelial cell seeding.

In 2005, Boura, *et al.* [52] evaluated the adhesion properties of endothelial cells (ECs) on two types of polyelectrolyte films ending either by poly(D-lysine) (PDL), or poly(allylamine hydrochloride) (PAH), and compared them to the data obtained on PDL or PAH monolayers, glass and fibronectin (Fn)-coated glass. ECs seeded on polyelectrolyte films showed a good morphology, allowing ECs to resist physiological shear stress better compared to ECs seeded on glass or Fn. Finally, PAH ending films improve strongly ECs adhesion without disturbing the adhesion mechanism, necessary for the development of a new endothelium.

In 2004, Zhu, *et al.* [53] formed thin polymer films of poly(ethylenimine)/alginate and alginate/poly-L-lysine (PLL) on activated poly-(DL-lactide) (PDL-LA) using the LBL technique to promote the chondrocyte cytocompatibility. The multilayer-modified PDL-LA films were investigated by X-ray photoelectron spectroscopy, attenuated total reflection FTIR, contact angle measurements and atomic force microscopy. The result of chondrocyte culture on

modified PDL-LA film, especially on the alginate/PLL multilayer, had much normal spreading morphology than that of PDL-LA virgin film. This study has demonstrated that the LBL of biomacromolecules multilayer on synthetic biodegradable polymer might have potentials for drug delivery, tissue engineering and other biomedical applications.

In 2005, Köstler, *et al.* [54] fabricated poly(diallyldimethylammonium chloride (PDADMAC)/PSS multilayer films on pretreated polymeric (PET and PTFE) and inorganic (glass slide and silicon wafer) substrates. Contact angle measurements showed a regular odd-even pattern even for the first PDADMAC/PSS layers on sufficiently smooth and hydrophilic substrates. The surface thermodynamic data indicated an increase in coating density with increasing layer number. The effect of thicker layers and a more coiled conformation by deposition from salt-containing solution were also noted by surface thermodynamic component. In the same year, Kolasinśka, *et al.* [55] prepared multilayer films of PAH/PSS using the layer-by-layer deposition technique on various support materials. Periodic oscillations in contact angle values were observed for the multilayer terminated by PAH and PSS, respectively and the variations in contact angle values strongly depended on the adsorption conditions and multilayer treatment after deposition. The optimum ionic strength of polyelectrolyte solution was used for deposition on wetting of multilayer films. PEI was modified as a first layer of PAH/PSS multilayer film to investigate the influence of the first layer.

In 2006, Lin, *et al.* [56] modified the poly(L-lactide) (PLLA) surface via electrostatic self-assembly of PAH and PSS. The process of layer growth was monitored by X-ray photoelectron spectroscopy (XPS) and contact angle measurements. These modified PLLAs were incorporated with gelatin to improve their cytocompatibility. The results showed that the PAH and PSS modified PLLA exhibited better cytocompatibility than virgin PLLA, and the incorporation of the gelatin on modified PLLA substrates improved their cytocompatibility.

In view of alternate LBL assembly of cationic chitosan with oppositely charged polyelectrolytes, the following related publications have been reported.

In 2000, Serizawa, *et al.* [35] studied the alternating anti-vs procoagulation activity of ultrathin polymer films prepared by the layer-by-layer assembly technique against human blood. Dextran sulfate (Dex) and chitosan were selected as polymers with anti- and pro-coagulation activities, respectively. The layer-by-layer assembly of these polymers was quantitatively analyzed by a quartz crystal microbalance (QCM). They also investigated the influence of salt concentration in the polymer aqueous solutions on the assembly process, which ultimately led to thicker films. This study demonstrated that biocompatibility of multilayers can be controlled. In 2002, Serizawa, *et al.* [36] continued their study on multilayer systems. They varied concentration of NaCl as 0.2, 0.5 and 1 M. They found that the apparent film thickness increased upon increasing NaCl concentration. There was a critical concentration for the alternating activity; above a concentration of 0.5 M NaCl, both anti- and pro-coagulation could be observed on the dextran sulfate and chitosan surfaces, respectively. They also studied the formation of assembled film from a combination of chitosan and heparin, but the activity was different from that of the former system. They suggested that the polymer species and/or the assembly conditions are key factors for realizing the alternating bioactivities of films prepared by the layer-by-layer assembly. Later in 2003, Serizawa, *et al.* [57] analyzed the gene expression of the alternating compatibility of fibroblast cells adhering to multilayers of chitosan and dextran sulfate (Dex) on a substrate. It was found that analysis of gene expression was a powerful tool for evaluating the bioactivity of multilayers.

In 2003, Zhu, *et al.* [58] modified poly(L-lactic acid) (PLLA) surface via aminolyzed the ester groups with diamine and constructed multilayer films using poly(styrene sulfonate, sodium salt) (PSS) and chitosan. The layer-by-layer deposition process was monitored by UV-vis spectroscopy, fluorescence spectroscopy, and contact angle. The PLLA membranes deposited with three or five bilayers of PSS and chitosan with chitosan as the outermost layer has better cytocompatibility.

In 2004, Feng, *et al.* [59] fabricated the polyelectrolyte complex multilayer of hyaluronic acid (HA)/chitosan with two different strategies and characterized by atomic force microscopy (AFM). With the first strategy, while the mica was rich in negative charges, chitosan was fabricated first and the HA were fabricated secondly. The films exhibited cluster features on the substrate. With the second strategy, while the mica was modified to be in positive charges, HA was fabricated first and chitosan was fabricated secondly. The films exhibited a more homogeneous feature and a nice miscibility at nanometer scale and had a lower roughness than pure chitosan films. The self-assembly polyelectrolyte complex films by strategy two were smoother and more uniform than the ones by strategy one.

In 2005, Cai, *et al.* [43] constructed a multilayer film assembly with chitosan (Chi) and gelatin (Gel) on titanium films in order to improve their biocompatibility via the layer-by-layer (LBL) technique. The LBL film growth was monitored by X-ray photoelectron spectroscopy (XPS), atomic force microscopy (AFM), confocal laser scanning microscopy (CLSM) and water contact angle measurement. *In vitro* cell viability showed that the Chi/Gel-modified films have higher cell viability than titanium films. Chi/Gel can thus be employed to surface engineer titanium via LBL technique.

In 2005, Fu, *et al.* [60] constructed heparin (anti-adhesive agent) and chitosan (antibacterial agent) multilayer films on aminolyzed PET films. The contact angle and UV results verified the progressive buildup the multilayer film by alternate deposition of the electrolyte. The properties of films were investigated by contact angle, atomic force microscopy (AFM), lateral force microscopy (LFM) and UV spectroscopy. The multilayer films not only reduced the bacterial adhesion but also kill the bacterial adhered onto the surface, which is very desirable to create a powerful anti-infection coating for cardiovascular devices. The assembly pH represented the important influence on both surface properties of the films, i.e., the composition, roughness, wettability and their anti-adhesive and antibacterial properties.



In 2005, Liu, *et al.* [61] modified a surface of poly(ethylene terephthalate) by hydrolysis and prepared multilayer films assembly with chitosan and chondroitin sulfate (CS) by the layer-by-layer (LBL) technique (Figure 2.4). The process of layer growth and oscillation of surface wettability were monitored by UV-vis spectroscopy and water contact angle, respectively. The *in vitro* culture revealed that the adherence of endothelial cells was enhanced on the biomacromolecules-modified PET film with their preserved function.

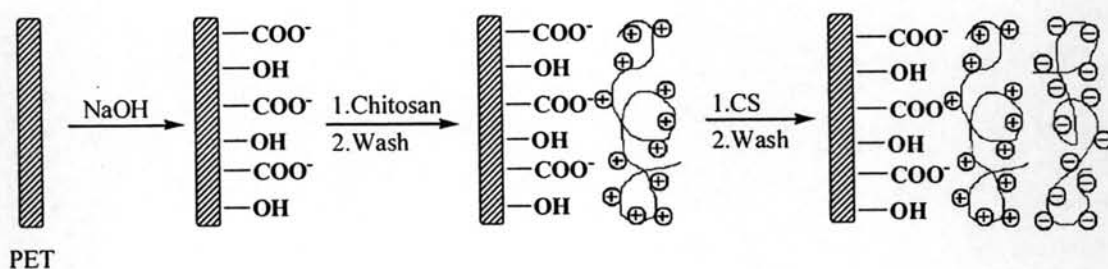


**Figure 2.4** schematic representations showing the introduction of carboxyl groups on PET surface by hydrolysis, and the layer-by-layer assembly with oppositely charged polyelectrolytes on the hydrolyzed PET film [61].

In our previous study [12], alternate bioactivity of the multilayer assembly of three pairs of polycation-polyanion (CHI-PSS, PAH-SFC, and HTACC-PAA) in the presence of 1 M NaCl on a plasma-treated PET substrates was tested against four proteins (albumin, fibrinogen,  $\gamma$ -globulin and lysozyme). It has been demonstrated that the proteins adsorbed on the assembled film in a multilayer fashion implying that the diffusion of the proteins within the multilayer has occurred. The fact that both HTACC and SFC are soluble in a broader pH ranges than possesses different bioactivities from chitosan.

## 2.6 Surface Characterization

### 2.6.1 Quartz Crystal Microbalance (QCM)

The signal transduction mechanism of the QCM technique relies upon the piezoelectric effect in quartz crystals, first discovered in 1880 by Jacques and Pierre, via a pressure effect on quartz. In 1959, the QCM was first used in a sensing mode when Sauerbrey [64] reported a linear relationship between the resonance frequency ( $F$ ) decrease of an oscillating quartz crystal and the bound elastic mass of deposited metal. Early chemical applications of QCM were to measure mass binding from gas-phase species to the quartz surface. In the 1980s, a solution-based QCM has been developed as a new oscillator technology to measure changes in frequency that could be related to changes in viscosity and density in highly damping liquid media (Figure 2.5). The recent success of the QCM technique is due to its sensitive solution-surface interface measurement capability, as well as to characterize energy dissipative or viscoelastic behavior of the mass deposited upon the metal electrode surface of the quartz crystal. These features make QCM a very attractive technique in various fields of chemistry and biochemistry.

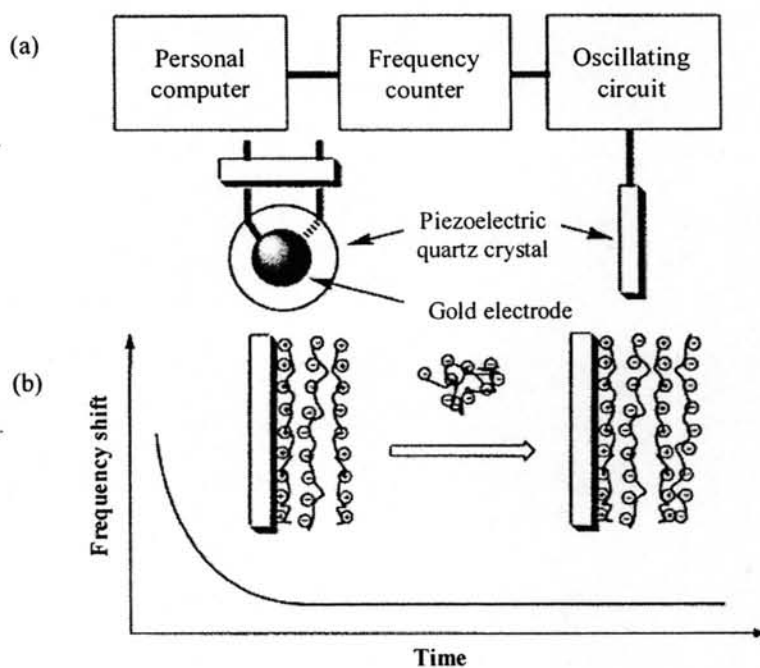


**Figure 2.5** (a) Schematic diagram of the QCM apparatus and (b) typical frequency-time domain plot of an in situ adsorption experiment [62].

Quartz is the most stable form of silica (or silicon dioxide  $\text{SiO}_2$ ). For the QCM applications, alpha-quartz crystals are employed, because of their superior mechanical and piezoelectric properties. The cut-angle with respect to crystal orientation determines the mode of oscillation. The AT cut crystal, which is the most commonly used for QCM applications, is fabricated by slicing through a quartz rod with a cut angle  $35^\circ 10'$  with respect to the optical axis, as shown in Figure 2.6, and this crystal performs a shear displacement perpendicular to the resonator surface. The advantage with the AT cut quartz crystal is that it has nearly zero frequency drift with temperature around room temperature.

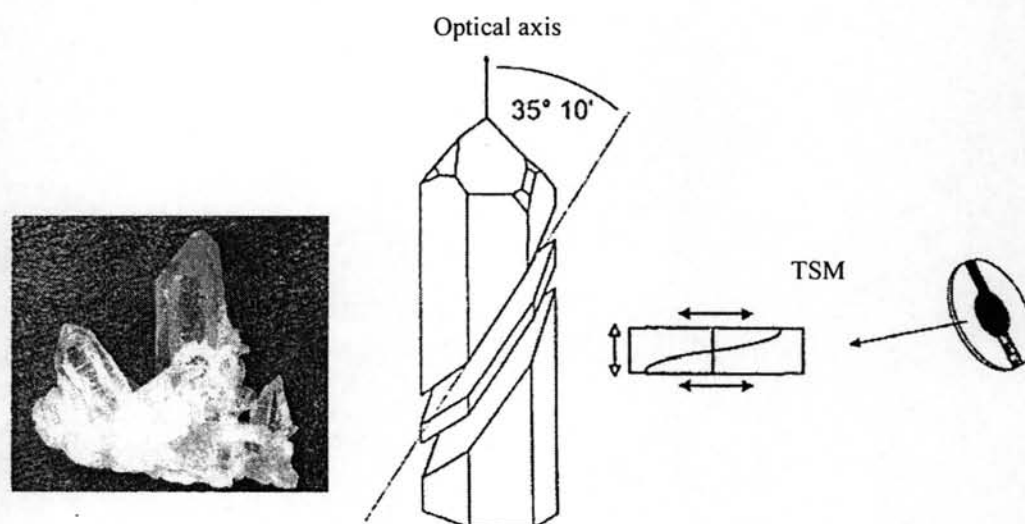


**Figure 2.6** The quartz crystal and AT-cut of a quartz crystal from which the metal coated QCM quartz crystals is produced and an end on crystal view of the thickness shear mode (TSM) of oscillation [63].

In the QCM studies we used a thin disk, sliced from single crystals of the alpha-quartz, which is sandwiched between two metal electrodes that are vapor deposited on either side of the crystal. Gold electrodes have been the most commonly used in QCM studies, because of the ease with which Au is evaporated. However, Cu, Ni, Pt and other metals have also been employed. Typical operating frequencies of the QCM lie within the range of 5 to 10 MHz.

The resonance frequency ( $F$ ) of the crystal depends on the total oscillating mass, including water coupled to the oscillation. When a thin film is attached to the sensor crystal, the frequency decreased. In this way, the QCM operates as a very sensitive balance. The mass of the adhering layer is calculated using the Sauerbrey equation [64] in Eq. (2.1). This equation is generally valid for measurements in air or in vacuum.

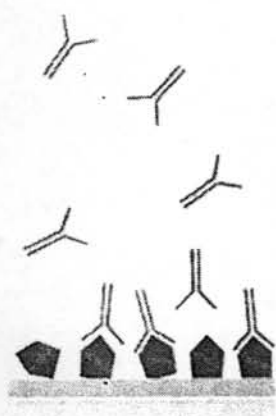
$$\Delta F = \frac{-2F_q^2 \Delta m}{A (\rho_q \mu_q)^{1/2}} \quad (2.1)$$

where	$\Delta F$	=	the change in resonant frequency (Hz)
	$F_q$	=	the fundamental resonant frequency of the quartz
	$\Delta m$	=	the change in elastic mass (g)
	$A$	=	the electrode area
	$\rho_q$	=	the density of quartz (2.65 g/cm <sup>3</sup> )
	$\mu_q$	=	the shear modulus of the quartz (2.95 x10 <sup>6</sup> N/cm <sup>2</sup> )

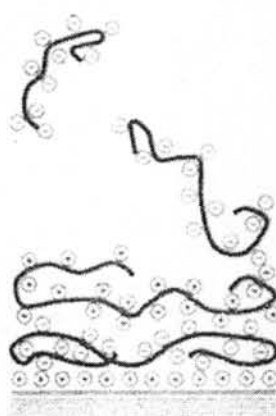
The QCM is a mass sensing device with the ability to measure very small mass changes on a quartz crystal resonator in real-time. The sensitivity of the QCM is approximately 100 times higher than an electronic fine balance with a sensitivity of 0.1  $\mu\text{g}$ . This means that QCM's are capable of measuring mass changes as small as a fraction of a monolayer or single layer of atoms. The high sensitivity and the real-time monitoring of mass changes on the sensor crystal make QCM a very attractive technique for a large range of applications as a sensor in:

- Electrochemistry of interfacial processes at electrode surfaces.
- Biotechnology:
  - Interactions of DNA and RNA with complementary stands,

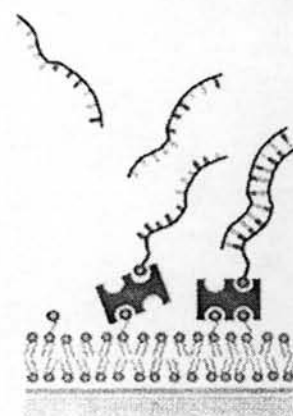
- Specific recognition of protein ligands by immobilized receptors, immunological reactions (Figure 2.7),
- Detection of virus capsids, bacteria, mammalian cells,
- Adhesion of cells, liposomes and proteins,
- Biocompatibility of surfaces,
- Formation and prevention of formation of biofilms,
- Thin film formation:
  - Langmuir and Langmuir-Blodgett films,
  - Spin coating,
  - Self-assembled monolayer,
  - Polyelectrolyte adsorption (Figure 2.7),



Proteins:  
adsorption/interaction



Polymers:  
multilayer formation



Lipids:  
biosensor templates

**Figure 2.7** Applications of QCM [65].

### 2.6.2 Contact Angle Measurement

One of the most sensitive methods known for obtaining surface tension information of solids is contact angle. This method is unique in that the equipment required is relatively simple and inexpensive. The basis of the measurement of solid surface tension by contact angle is the equilibrium of the three-phase boundary, shown in Figure 2.8 which can be described by Young's equation in Eq. (2.2). If the angle  $\theta$  is less than  $90^\circ$ , the liquid is said to wet the solid. If it is greater than  $90^\circ$ , it is said to be non-wetting. A zero contact angle represents complete wetting.

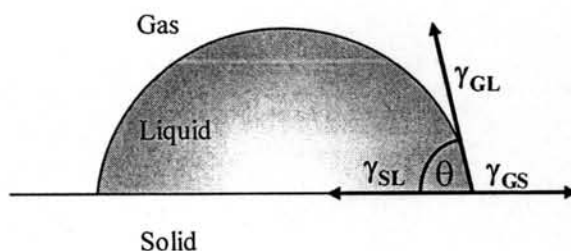


**Figure 2.8** Equilibrium of the three-phase boundary on solid surface [66].

$$\text{Young's Equation: } \gamma_{GS} - \gamma_{SL} = \gamma_{GL} \cos\theta \quad (2.2)$$

where

- $\gamma_{GL}$  = interfacial tension between gas phase and liquid phase
- $\gamma_{GS}$  = interfacial tension between gas phase and solid phase
- $\gamma_{SL}$  = interfacial tension between solid phase and liquid phase

The Young's equation applies for a perfectly homogeneous, atomically flat and rigid surface. In the case of real surfaces, the contact angle value is affected by surface roughness, heterogeneity, vapor spreading pressure, and chemical contamination of the wetting liquid. Although the technique to measure contact angles is easy, data interpretation is not straightforward and the nature of different

contributions to the surface is a matter of discussion. Generally, one can define the complete wetting, wetting, partial wetting, and non-wetting according to Figure 2.9.

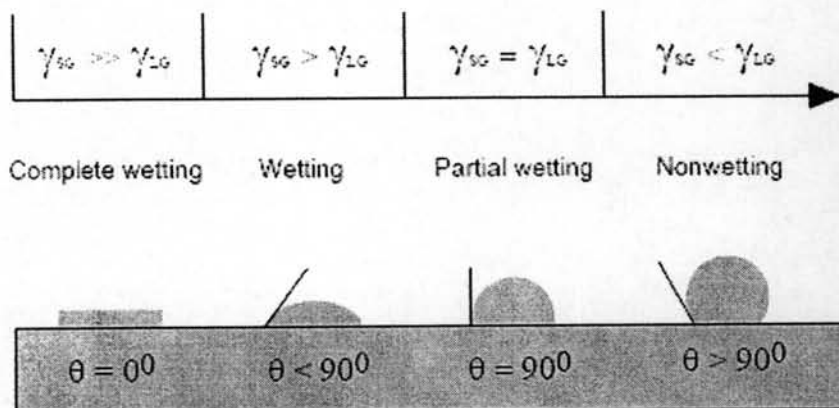


**Figure 2.9** Schematic representation of wettability [66].

In this research, air-water contact angle was used for determining the wettability and the stratification of multilayer films.

### 2.6.3 Attenuated Total Reflectance-Fourier Transform Infrared Spectroscopy (ATR-FTIR)

The infrared beam from the spectrometer is focused onto the beveled edge of an internal reflection element (IRE). The beam is then reflected, generally numerous times, through the IRE crystal, and directed to a detector (Figure 2.10).

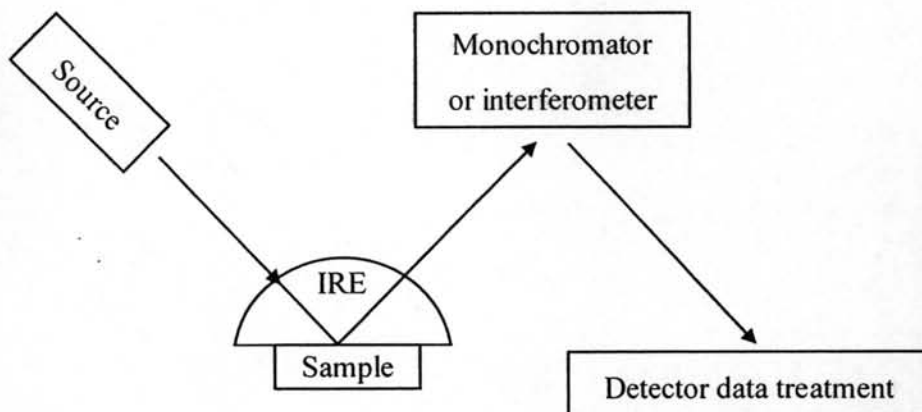


**Figure 2.10** Diagram of ATR-FTIR [67].

Typical materials used for ATR prism are Ge, Si and ZnSe. The infrared radiation can penetrate a short distance into the sample, thus interacts with any functionalities existing within that depth. The depth of penetration ( $d_p$ , defined as the distance from the IRE-sample interface where the intensity of the evanescent wave decays to  $1/e$  of its original value) can be calculated using the formula in Eq. (2.3):

$$d_p = \frac{\lambda}{2\pi n_p (\sin^2 \theta - n_{sp}^2)^{1/2}} \quad (2.3)$$

where

- $\lambda$  = wavelength of the radiation in the IRE
- $\theta$  = angle of incidence
- $n_{sp}$  = ratio of the refractive indices of the sample vs. IRE
- $n_p$  = refractive index of the IRE

In this study, ATR-FTIR was used for identifying functional groups on the surface of the films. Sampling depth of characterization is 1-1.5  $\mu\text{m}$ .



### 2.6.4 Scanning Probe Microscopy (SPM)

Scanning probe microscopy covers several related technologies for imaging and measuring surfaces on a fine scale, down to the level of molecules and groups of atoms. The development of SPM techniques, starting in the early 1980's, has revolutionized surface science and has had a huge impact on device technologies such as microelectronics, DVDs, and high-density magnetic recording.

SPM techniques share the concept of scanning an extremely sharp tip (3-50 nm radius of curvature) across the object surface. The tip is mounted on a flexible cantilever, allowing the tip to follow the surface profile as shown in Figure 2.11.

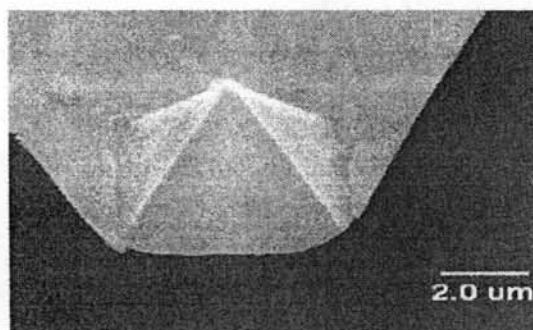


**Figure 2.11** A probe used for atomic force microscopy [68].

When the tip moves in proximity to the investigated object, forces of interaction between the tip and the surface influence the movement of the cantilever. These movements are detected by selective sensors. Various interactions can be studied depending on the mechanics of the probe.

#### **Probe Techniques**

The three most common scanning probe techniques are:

1. Atomic Force Microscopy (AFM) measures the interaction force between the tip and surface. The tip may be dragged across the surface, or may vibrate as it moves. The interaction force will depend on the nature of the sample, the probe tip and the distance between them as shown in Figure 2.12.

2. Scanning Tunneling Microscopy (STM) measures a weak electrical current flowing between tip and sample as they are held a very distance apart.

3. Near-Field Scanning Optical Microscopy (NSOM) scans a very small light source very close to the sample. Detection of this light energy forms the image. NSOM can provide resolution below that of the conventional light microscope. There are numerous variation of AFM techniques; AFM may operate in several modes that differ according to the force between the tip and surface.

### Tip-sample interaction

The way in which image contrast is obtained can be achieved in many ways. The three main classes of interaction are *contact mode*, *tapping mode* and *non-contact mode*.

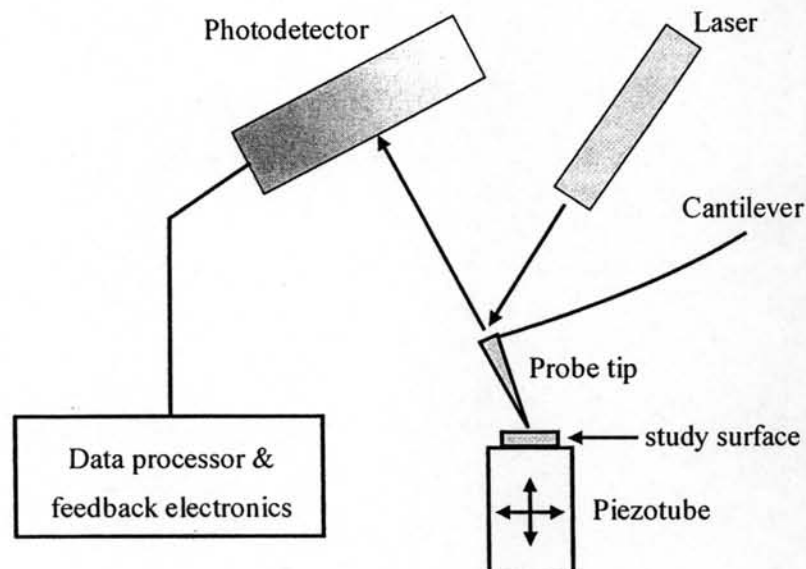
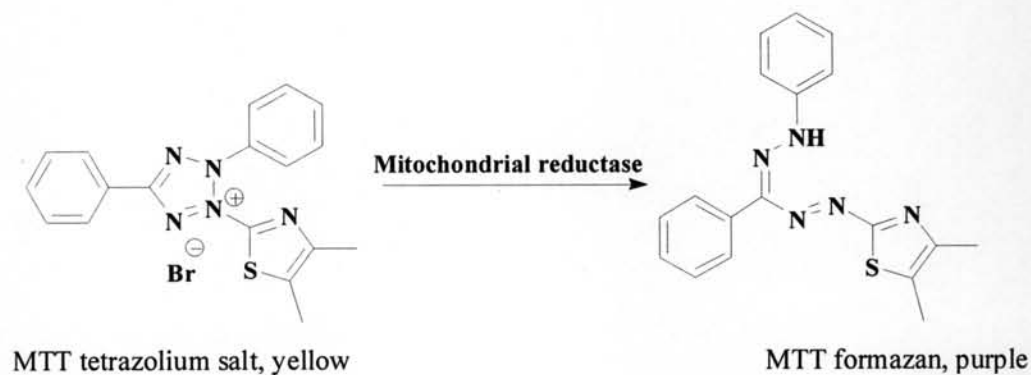


**Figure 2.12** Schematic diagram of AFM system showing the optical method of measuring cantilever deflection [69].

### 2.6.5 MTT Reduction Assay

MTT [3-(4,5-dimethylthiazol-2-yl)-2,5-diphenyltetrazolium bromide] assay, first described by Mosmann in 1983 [72], is based on the ability of a mitochondrial dehydrogenase enzyme from viable cells to cleave the tetrazolium rings of the pale yellow MTT and form a dark blue formazan crystals (Scheme 2.9) which is largely impermeable to cell membranes, thus resulting in its accumulation within healthy cells. Solubilization of the cells by the addition of a detergent results in the liberation of the crystals which are solubilized. The number of surviving cells is directly proportional to the level of the formazan product created. The color can then be quantified using a simple colorimetric assay.



**Scheme 2.9** Reduction of the MTT tetrazolium salt to formazan [70].

The MTT assay was used in many studies to evaluate the viability of different cells because this test is fast, many samples (up to 10) can be examined at the same time and many replications of each sample can be performed simultaneously.